



HAL
open science

Assessing goats fecal avoidance using image analysis based monitoring

Mathieu Bonneau, Xavier Godard, Jean-Christophe Bambou

► **To cite this version:**

Mathieu Bonneau, Xavier Godard, Jean-Christophe Bambou. Assessing goats fecal avoidance using image analysis based monitoring. 2021. hal-03402714

HAL Id: hal-03402714

<https://hal.inrae.fr/hal-03402714>

Preprint submitted on 25 Oct 2021

HAL is a multi-disciplinary open access archive for the deposit and dissemination of scientific research documents, whether they are published or not. The documents may come from teaching and research institutions in France or abroad, or from public or private research centers.

L'archive ouverte pluridisciplinaire **HAL**, est destinée au dépôt et à la diffusion de documents scientifiques de niveau recherche, publiés ou non, émanant des établissements d'enseignement et de recherche français ou étrangers, des laboratoires publics ou privés.



Distributed under a Creative Commons Attribution - NonCommercial - NoDerivatives 4.0 International License

Assessing goats fecal avoidance using image analysis based monitoring

Mathieu Bonneau^{1,*}, Xavier Godard², and Jean-Christophe Bambou¹

¹URZ Zootechnique Research, INRAE, Petit-Bourg (Guadeloupe), France

²UE PTEA Tropical Platform for Animal Experimentation, INRAE, Petit-Bourg (Guadeloupe), France

Correspondence*:

INRAE URZ, domaine Duclos, 97129 Petit-Bourg, Guadeloupe
mathieu.bonneau@inrae.fr

2 ABSTRACT

3 The recent advances in sensor technologies and data analysis could improve our capacity to
4 acquire long term and individual dataset on animal behavior. This is particularly interesting when
5 behavioral data could be linked to zootechnical, physiological or genetical information, with the
6 objective of improving animal management. In this article we proposed a framework, based on
7 computer vision and deep-learning, to automatically estimate animal location inside pasture. We
8 illustrated our framework for the monitoring of grazing goats. We were able to detect, in average,
9 87.95% of the goats and to identify the detected individuals with an average sensitivity of 94.9%
10 and an average precision of 94.8%. Goats were allowed to graze an experimental plot, where
11 infected feces with gastro-intestinal nematodes were previously dropped in delimited areas. Four
12 animals were monitored, during two grazing weeks on the same pasture (Try 1 and Try 2), spaced
13 from more than 2 months. Using the monitoring framework, we were able to study different aspect
14 of animal behavior, relating to parasitology. First, we monitored the ability of the animal to avoid
15 feces on pasture, and showed an important temporal and individual variability. Interestingly, the
16 avoidance capacity of all animals increased during the second grazing week (Try 2), and the level
17 of increase was correlated to the level of infection during Try 1. We also studied the relationship
18 between the time spent on contaminated areas with the level of infection, and was not able to
19 find clear relationship. We characterized social behavior using the inter-individual distance, but
20 again, we were not able to find a link with the level of infection. Due to the low number of studied
21 animals, biological results have to be interpreted with caution, but our framework can be used to
22 explore the relationship between behavior and parasitism in routine experimentations.

23 **Keywords:** image analysis, parasitism, animal behavior, feces avoidance, creole goats

1 INTRODUCTION

24 Goats are an important resource mainly for meat and milk production. In 2019, the number of farmed
25 animals was estimated to be more than 870 millions (<http://www.fao.org/faostat>), with approximately 94%
26 of the animals located in Asia and Africa. Infection to gastro-intestinal nematodes (GIN) is the number
27 one health constraint and is responsible for reduced production and increased mortality, especially for
28 the young and adult females, during the periparturient period. There exists different species of GIN, the
29 most important being *Haemonchus contortus*, known as the barber pole. Adult worms are located inside
30 the abomasum and an adult female can release from 5 to 10,000 eggs on the pasture daily. *Haemonchus*

31 *contortus* is blood feeding and heavy infection can results in anemia. In the past, GIN management
32 successfully relied on systematic anthelmintic (AH) treatment. Unfortunately, resistant nematodes to AH
33 was gradually selected (Kaplan and Vidyashankar, 2012) and it is now admitted that relying only on AH is
34 not a sustainable strategy (Charlier et al., 2018).

35 There exists several alternatives to manage GIN infection in small ruminants, most of them relying on
36 prevention. For example with genetic selection of resistant animals or with optimal pasture management
37 to limit the number of GIN on pasture during grazing. Modelling is an important tool to understand the
38 interactions between the alternative management options, and could be used to design sustainable strategies,
39 adapted to the farmer's constraints. This requires a good understanding of the GIN population dynamic and
40 to predict the impact of management. Models of GIN population dynamic on pasture (Rose et al., 2015) or
41 inside the host (Louie et al., 2005; Saccareau et al., 2016) are available in the literature, but the dynamic
42 of GIN ingestion, i.e. timing and quantity of ingested GIN, is not well described. However, accounting
43 for the dynamic of GIN ingestion and for individual variability can have important impact on the entire
44 GIN population dynamic (Cornell et al., 2004; Fox et al., 2013; Bonneau et al., 2018). Modelling ingestion
45 is a difficult task, mainly because it is difficult to estimate the spatial distribution of GIN on pasture and
46 the number of GIN included in each bite. The recent developments in precision livestock farming tools
47 offer new opportunities, especially to characterize animal behavior, and to study the relationship with GIN
48 infection.

49 Most of the studies considering the relationship between animal behavior and GIN infection were on
50 the capacity of the animal to avoid feces. To the best of our knowledge, all the studies relied on visual
51 observations, either directly or from video recording, and most of them were for sheep. In particular,
52 several studies found that sheeps were able to avoid feces during grazing (Hutchings et al., 2006), that the
53 avoidance level was greater for the infected animals (Hutchings et al., 1999; Cooper et al., 2000), and that
54 the avoidance level decreased with the age of feces (Hutchings et al., 1998). For goat, we were aware of
55 only one study (Brambilla et al., 2013), which underlined the fecal avoidance capacity of wild *Alpine Ibex*.
56 However, they did not found a relationship between avoidance and infection level. Dominance status can
57 influence the animal diet, with the dominant animals having the opportunity to be more selective (Barroso
58 et al., 2000), and thus potentially avoid more easily the infected areas. We found only one article that
59 studied the relationship between social behavior and GIN infection in goat (Ungerfeld and Correa, 2007).
60 They found that the most dominant goats had a fecal egg count (FEC), i.e. the number of GIN eggs per
61 gram of feces, significantly lower.

62 In this article, we proposed an experimental framework to study the relationship between animal behavior
63 and GIN infection. We designed a pasture where the quantity and location of infected feces were known. A
64 group of four animals were released on the pasture and monitored during one week to estimate the time
65 spent inside infected and non-infected areas. The first objective was to study the ability of the goats to
66 avoid feces. The second objective was to study the relationship between the time spent on infected areas
67 and the animal level of infection after grazing. The third objective was to study the relationship between
68 social behavior and GIN infection. The experimental framework is based on automatic monitoring of the
69 animals using image analysis (Li et al., 2021). Convolutional neural networks (CNN) are generally the
70 most adapted image analysis method and has been used successfully, mostly for pigs (Yang et al., 2019;
71 Zhang et al., 2019; Marsot et al., 2020; Zheng et al., 2020; Gan et al., 2021), but also for goats (Wang et al.,
72 2018; Bonneau et al., 2020; Jiang et al., 2020; Su et al., 2021). Several methods for cattle monitoring also
73 successfully identified animals using deep-learning technics (Andrew et al., 2017; Qiao et al., 2019; Achour
74 et al., 2020). The main advantage of using CNN is that powerful models, trained on millions of images and

75 designed by research teams with relevant engineering skills, are available free of charge. Then, new users
76 can almost directly use these CNN, just by retraining some parameters in order to be able to detect and
77 classify their objects of interest. In this article, we proposed to use Yolo associated with resNet-50 to detect
78 and identify the animals.

2 MATERIAL AND METHODS

79 2.1 Experimental setup

80 The aim of the experiment was to monitor animals during a natural GIN infection. To control GIN
81 infection, the animals were allowed to graze on a contaminated pasture during one week. Before and after
82 grazing, the animal was maintained in a worm-free environment, in order to guaranty that infection can
83 only occurred during grazing.

84 The experiment was decomposed into three stages. The first stage, is a worm-free environment stage,
85 where the worm burden of each animal is controlled and maintained to zeros. The second stage is the
86 grazing stage, where the animals are exposed to GIN during grazing. The third stage, is a worm-free
87 environment stage, where the GIN level of infection due to contamination in the second stage is assessed.

88 We repeated the experiment two times, in *Try 1* and *Try 2*, with 2 months and 16 days between the two
89 tries. The same pasture and animals were used for the two tries.

90 All the experiments were conducted at the INRA-PTEA experimental facilities located in Guadeloupe.

91 Illustrations and schematic representation of the experiment are available in figure 1.

92 2.1.1 Animals

93 Four male Creole goats were selected to maximize color differences between individuals. The first goat,
94 referred as *white*, weighted 34.13kg and was 16 months old at the beginning of the experiment. It had
95 black coat with white color patches on the belly. The second goat, referred as *brown*, weighted 33.93kg
96 and was 12 months and 17 days old at the beginning of the experiment. It has brown coat with a black strip
97 on the back. The third goat, referred as *black*, weighted 31.62kg kg and was 12 months and 17 days old at
98 the beginning of the experiment. It had homogeneous black coat. The last goat, referred as *red*, weighted
99 39.92kg and was 12 months and 11 days old at the beginning of the experiment. It had reddish brown coat
100 with a black strip on the back.

101 2.1.2 Stage 1 and stage 3: worm free environment

102 The animal were drenched with cydectine 0.1% at the beginning of the first try and with biaminthic 5% for
103 the second try. To control the efficacy of the anthelmintic treatment, we assessed the FEC one week before
104 grazing. For the second try, we observed that animals still had non zeros FEC and they were drenched a
105 second time. The individual FEC was re-assessed on the first grazing day, to confirm that animals were
106 worm-free. In any case, the anthelmintic treatment was gave more than 6 days before grazing in order to
107 avoid anthelmintic remanence. To assess the individual FEC, approximately 5g of feces were collected
108 from the rectum and directly transported to the laboratory using plastic tubes to avoid contamination. The
109 feces samples were analyzed individually using a modified McMaster technic. The FEC was expressed as
110 the number of eggs per gram of feces (Aumont et al., 1997). Before and after grazing, the animals were
111 maintained together in a stall and were fed with dry hay to avoid parasite ingestion outside of the grazing
112 week. After grazing, FEC was assessed at least every week, starting 8 days after grazing. FEC is a common

113 proxy of the animal worm burden, it makes the hypothesis that the number of eggs in the feces increases
 114 with the number of parasites inside the host. Although in general the animals with the highest FEC are also
 115 the animals with the highest worm burden, this might not be true in some extreme cases (Bishop and Stear,
 116 2000).

117 2.1.3 Stage 2: Grazing

118 We designed a square pasture of 144m², with a semi-closed adjacent area of 9m², equipped with water.
 119 This area was used by the animals to rest and to be protected from the rain and sun. To define the infected
 120 areas, we delimited two rectangles of 2m×6m=12m² each. The areas were delimited with metallic bars
 121 sunk into the ground, with only 20cm of the bar above the ground, to avoid disrupting animal behavior.
 122 The pasture was approximately flat, to limit GIN movement on pasture due to water flow.

123 The pasture was worm free before the experiment and was mowed approximately 1 month before the
 124 beginning of grazing on Try 1. When grazing started, grass was in average 7.32cm (n=22) in the non
 125 infected areas, 8cm (n=8) in the first infected area and 8.3cm (n=9) in the second. At the end of grazing on
 126 Try 1, grass was mowed at ground level in order to limit the persistence of parasites on the infected areas.
 127 20 days before grazing on Try 2, grass and ground samples were collected in the infected and non-infected
 128 areas in order to guarantee that parasites were not present on pasture. We used a Baerman technic to extract
 129 parasites from the samples and was not able to detect any gastro-intestinal nematodes. When grazing starts
 130 on Try 2, the grass was in average 10.7cm (n=23) in the non-infected area, 10.8cm (n=11) in the first
 131 infected area and 9.3cm (n=12) in the second infected area.

132 900g of infected feces were dropped homogeneously inside each of the infected area. Feces were dropped
 133 manually 13 days before grazing on Try 1 and 10 days before grazing on Try 2, expecting to maximise
 134 the number of infected larvae on pasture during grazing. On Try 1, feces were obtained from 10 naturally
 135 infected animals. The feces were mixed homogeneously and FEC was estimated from 10 different samples
 136 (mean FEC = 576 eggs/g, std = 265 eggs/g). On Try 2, feces were obtained from 16 experimentally infected
 137 animals. FEC was assessed for each animals (mean FEC = 4431 eggs/g, std = 43.8 eggs/g) and feces was
 138 mixed together homogeneously.

139 In order to estimate the number of larvae on the infected areas, 6 control feces samples of 80g each were
 140 dropped in 30cm square quadrats, outside of pasture. Two grass samples were then collected from two
 141 quadrats, on the 1st, 3rd and 6th grazing days for Try 1, and on the 1st, 3rd and last grazing days for Try 2.
 142 The number of infected larvae was then estimated with a Baerman technic. We averaged the number of
 143 larvae found from the two control samples to extrapolate the number of larvae present in the infected areas,
 144 from the 900g of feces:

$$n_{L3}^p = \frac{n_{L3}^{c1} + n_{L3}^{c2}}{2} \times \frac{900}{80}.$$

145 Where n_{L3}^p is the estimated number of larvae inside an infected area, n_{L3}^{c1} and n_{L3}^{c2} are the number of larvae
 146 found in the first and second control samples.

147 2.1.4 Recording with time-lapse cameras

148 We used a construction time-lapse cameras (Brinno TLC2000 pro 2018), equipped with waterproof
 149 plastic protection. The camera records at 1.3 Mpx with a resolution of 1208 × 720 using jpeg compression.
 150 It was setup to take one picture every 20s from 6:30 to 18:00. When we controlled the images acquired
 151 during Try 1, we realized that the camera was facing the sun during sunrise, which decreases the quality of
 152 the images. As a consequence, the location of the camera was adapted accordingly for Try 2 (see figure 1).

153 2.2 Animal monitoring

154 We developed an algorithm to analyze each image of the time-lapse camera independently. The algorithm
155 was decomposed into two steps: (i) to detect the animals on the picture, and (ii) to estimate the identity of
156 the animal, i.e. white, brown, black or red.

157 2.2.1 Animal detection

158 To detect animals, we used a common approach, based on the CNN Yolo v2 (Redmon and Farhadi, 2017),
159 which is known to run fast, with high accuracy and high learning capacities.

160 Yolo divides the image into grid cells of various sizes and predicts what objects are present into each cell.
161 Then a combination of different technics allow to find back the exact bounding boxes around the detected
162 objects, by reasoning on the global image. For image feature extraction, Yolo can be used with classical
163 CNNs for image classification. For our purpose, we trained one version of Yolo, based on inception v3
164 (Szegedy et al., 2016) and another version based on resNet-50 (He et al., 2016). Each network was trained
165 on the same set of 3,820 images where the goats were manually labelled. We performed an empirical
166 evaluation of the two networks and found that the architecture based on resNet provided better results.

167 In very few cases, Yolo returned more than 4 detections, mostly when multiple bounding boxes was
168 associated to the same animal. When more than four bounding boxes was found, we simply used a non-max
169 suppression method to remove the overlapping bounding boxes, and selected the four bounding boxes with
170 the highest probability.

171 The detections inside the resting area were not accounted for.

172 2.2.2 Individual identification

173 The results of the Yolo detection stage is a set of bounding boxes, $(x_a, y_a, w_a, h_a)_{a=1\dots n}$, around the
174 detected animals, where x_a and y_a are the column and row numbers of the top left corner of the bounding
175 box number a . w_a and h_a are the width and height of the bounding box, and n is the number of bounding
176 boxes/detected animals. From the original image, we then extracted n sub-images, corresponding to the
177 bounding boxes, and move to the next step: identify the animal inside each bounding box.

178 This second step is an image classification problem, with 4 different classes, *white goat*, *brown goat*,
179 *black goat* and *red goat*. There is several CNN that are available free of charge, and trained on more than
180 one million of images to perform image classification. Even though these CNNs are generally trained to
181 recognize common objects such as dogs, stop signs or humans, their architecture and most of their layers
182 can be directly used to recognize new classes, which is known as transfert learning. This is due to the
183 quality of their architecture to extract useful features from images.

184 We also tested two different CNNs, resNet-50 and inceptionV3. In each case, only the parameters of
185 the last 10 layers were re-trained. When labelling the training images for Yolo, we also labeled the color
186 of the animals. We thus used the 3,200 training images labeled for Yolo, to extract 12,236 images with
187 color labels. In total, approximately 3,400 images were available for the white goat and 2,900 images for
188 the other goats. 70% of the dataset was used to retrain the CNNs and 30% to evaluate their performance.
189 resNet-50 provided higher sensitivity and precision values, and was used for the analysis.

190 Compared to other image classification problem, we had an extra information, two detections cannot be in
191 the same class. Instead of directly using the prediction of the CNN, we used it to compute the probability of
192 each bounding box being from an animal of the four different color. For each bounding box (x_a, y_a, w_a, h_a) ,

193 the CNN associated a set of probabilities ($p_{\text{white}}^a, p_{\text{brown}}^a, p_{\text{red}}^a, p_{\text{red}}^a$). A score was then calculated for each
 194 possible color configuration of the bounding boxes. If c^a is the color of the bounding box number a , the
 195 score of a configuration (c^1, \dots, c^n) is simply the sum of the probabilities of the bounding boxes to be in
 196 that colors:

$$V(c^1, \dots, c^n) = \sum_{a=1}^n p_{c^a}^a.$$

197 We finally chose the color configuration with the highest score.

198 2.2.3 Evaluation

199 To evaluate the capacity of the method to detect and identify animals, we designed a MATLAB
 200 application, which selected randomly an image on the data bank and displayed the detected animals
 201 and their identifications. For each color (i.e. white, brown, black and red), the user first selected if the
 202 animal was detected, non-detected or absent (i.e. inside the resting area). When the animal was detected,
 203 the user also had to select the detected color. A second script was designed to manually record the location
 204 of the missed detection.

205 We ran the application to control more than 600 images for each try. In order to assess the capacity of
 206 the method to detect the animals, we computed the percentage of detected animals. For each color, the
 207 percentage of detection is equals to $100 * (\frac{nbD}{nbD+nbND})$. Where nbD is the number of images where the
 208 animal is detected and $nbND$ is the number of images where the animal is not detected.

209 In order to assess the capacity of the method to identify the animals, we compared the estimated and true
 210 color of each detection. Then we evaluated the sensitivity and precision for each color class.

211 2.3 Animal Behavior

212 2.3.1 Avoidance capacity

213 To characterize the capacity of the animals to avoid infected areas, we computed the number of times
 214 each animal was detected on the infected, and non infected areas. In order to be able to compare the two
 215 quantities, the number of detection was normalized by the surface area of each zone, which provides a
 216 number of detection per m^2 . Finally, we defined the avoidance index as the ratio of the number of detection
 217 per m^2 inside the non-infected and the infected areas:

$$\text{Avoidance Index} = \frac{d^{nia}/120}{d^{ia}/24}.$$

218 Where d^{nia} is the number of detection inside the non infected area and d^{ia} is the number of detection
 219 inside the two infected areas. We recall that the non infected area is $120m^2$ and the infected areas is
 220 $2 \times 12 = 24m^2$.

221 An avoidance index > 1 means that the number of detections per m^2 is strictly higher for the non-infected
 222 area. The greater is the avoidance index, the greater is the feces avoidance.

223 We computed a daily avoidance index, where d^{nia} and d^{ia} were computed daily. We also computed the
 224 weekly avoidance index, where d^{nia} and d^{ia} were computed over the entire grazing week.

225 2.3.2 Larval exposure and FEC

226 We explored the relationship between the time spent on infected areas, the number of larvae on pasture
227 and the animal's FEC after grazing.

228 To quantify the individual grazing time inside the infected areas, we first calculated the proportion of
229 time each animal spent in these areas, which was easily obtained from the animal monitoring framework.
230 Then, we simply extrapolated the amount of time, in minutes, on the entire day, from sunrise to sunset.

231 To quantify the daily quantity of larvae inside the pasture, we first computed a linear interpolation of the
232 number of larvae inside the two infected areas during the 7 grazing days. The linear interpolation consisted
233 in connecting two observations with a straight line.

234 To summarize these two informations, we defined the exposure index, as the sum of the daily products
235 between the grazing time inside the infected areas and the number of larvae. For an animal, the exposure
236 index is thus:

$$\text{Exposure Index} = \sum_{t=1}^7 (p_{ia}^t * t_{\text{Daylight}}) \times nl^t.$$

237 Where p_{ia}^t is the proportion of time spent inside infected areas during day t , t_{Daylight} is the daylight duration,
238 in minutes. And nl^t is the number of estimated larvae, inside the two infected areas, on day t .

239 We defined the exposure index to quantify animal exposure to larvae, it is monotonically increasing with
240 the quantity of larvae available on pasture and the time spent on infected areas.

241 A better approximation of nl^t should take into account the quantity of larvae that has been ingested by
242 the animals during grazing. Unfortunately, this quantity is hardly predictable.

243 Finally, in order to express the animal level of infection, we used the logarithm of the area under the
244 FEC curve (LAF) of each animal. The area under the FEC curve is a useful information as it allows
245 characterizing the infection over the entire infection period. We used the logarithm for clarity of the
246 graphical representation.

247 2.4 Social Distance

248 The inter-individual distance is a good indicator of the dominance relationship between the animals
249 (Aschwanden et al., 2008). To reduce the risk of aggressive behavior from the dominant animals, subordinate
250 animals tend to be more distant from the dominant ones. To characterize the distance between the detected
251 animals, we first used a geometric transformation to transform the coordinates of the detected animals, in
252 pixels, to spatial coordinates. Then, we estimated the spatial coordinates of the animals center of gravity on
253 the pasture ground.

254 The location of the detected animal in the image was derived from the bounding boxes estimated by Yolo.
255 It is particularly complicated to project the center of gravity of the animal on the pasture ground, because it
256 can take many different postures and can be located at various angles from the camera. As in Bonneau et al.
257 (2020), we used the following approximation:

$$(ppx, ppy) = \left(px + \frac{w}{2}, py + 0.9 * h \right).$$

258 Where (px, py) are the coordinates, in pixels, of the bounding box top left corner, (w, h) are the width and
259 height of the bounding box and (ppx, ppy) are the coordinates, in pixels, of the estimated projection on the
260 pasture ground.

261 In order to estimate the geometric transformation from pixels to spatial coordinates, 16 marks were setup
262 on the pasture grounds (see figure 4). We used the 8 corners of the infected areas, the 4 corners of the pen,
263 and the 4 middles of the pen on each side of the pasture. Marks were then manually identified on the image
264 to calculate their coordinates in pixels. The spatial coordinates of the marks were easily know, according
265 to the dimension of the pen and of the infected areas. We estimated the relationship between the marks
266 coordinates in pixels and in spatial coordinates by fitting a projective transformation. The transformation
267 was then use to estimate the spatial coordinates of the detected animals. The conversion of pixels in image
268 to spatial coordinates in real world is known as an image registration problem (Zitova and Flusser, 2003).

269 Finally, for each image, we computed the inter-individual distance between each detected animals, based
270 on their estimated spatial coordinates.

3 RESULTS

271 3.1 Sward height

272 The sward height at the start and at the end of the grazing week is available Table 1. For both try, grass
273 intake was relatively similar inside the first infected area and the non-infected area. Grass intake was lower
274 inside the second infected area, which is explained by a small patch of non-grazed grass (voir si on peut
275 aller savoir ce que c'était).

276 3.2 Number of larvae in the infected areas

277 The estimated number of larvae per infected areas is available figure 2. When grazing started, there were
278 more than 14,000 larvae available on the grass of each infected area. Surprisingly, in Try 2, where the feces
279 were much more infected than in Try 1, the number of available larvae is approximately the same at the
280 beginning. However, the population was increasing until grazing day 3 in Try 2, whereas it decreased in
281 Try 1. This was anticipated because the feces were dropped later in Try 2.

282 3.3 Post grazing worm burden

283 The individual fecal egg count (FEC) for the first and second try are available figure 3. The FEC stayed
284 relatively low ($< 4,000$) during the evaluation period of Try 1. The brown goat had the highest FEC value.
285 The black and white goat had relatively similar FEC values, close to 2,000 on the last FEC assessment. The
286 FEC of the red goat did not exceed 700 eggs/g, which corresponds to a benign infection. A voir avec JC.

287 For the second Try, the black goat got heavily infected with a maximal FEC value close to 17,000 eggs/g.
288 The number of excreted eggs was relatively similar for the white and brown goats, with a maximal value
289 close to 3,000 eggs/g. The red goat had an excretion pic ...

290 A reprendre avec JC.

291 3.4 Animal detection and identification

292 The percentage of animal detected is available in Table 2. In average, 86% of the goats were detected
293 during Try 1 and 89.9% during Try 2. The white goat had the highest detection rate. This goat had a white
294 coat patches on the belly, which is highly discriminant and certainly helped the detection and identification

295 algorithms. The brown and black goats had similar detection rates, whereas the brown goat was the one
296 with the lowest detection rate. As shown on figure 4, most of the missed detections were located on the
297 opposite side of the camera. We also noted that missed detection can occurred when the goats were close
298 from each other. In this case, only one goat was detected.

299 The sensitivity and precision of the animal identification method are available Table 3. The average
300 sensitivity was close to 95% for each try. We observed confusion between the brown and red goats, which
301 had similar tint. There was also some confusion between black and white goats, which had most of the
302 coat of black color. When the white coat patches on the belly was not visible, the identification method
303 recognized the white goat as the black one. As for the detection method, we observed a better sensitivity
304 and precision during Try2. During this try, the camera was never facing the sun, which increased the image
305 quality and as a consequence, the quality of the detection and identification methods.

306 As it is shown on figure 5, the number of missed detection is highest between 6:00 to 8:00 for Try 1.

307 **3.5 Avoidance capacity**

308 The daily and cumulated avoidance index for Try 1 and Try 2 are available figure 6.

309 During the first Try, the white and black goats favored the non-infected area during the first 3 grazing
310 days. From grazing day 4, they started to choose the infected areas rather than non-infected one. The
311 avoidance index of the red goat is lower than one only on days 4 and 7. The brown goat favored the infected
312 areas during the entire grazing week.

313 Over the entire grazing week, only the red goat had an avoidance index > 1 .

314 For the second Try, the black and red goats had an avoidance index > 1 during the entire grazing week.
315 Unlike during the first Try, the brown goat had an avoidance index ≥ 1 during the first 6 grazing days and
316 only favored the infected areas during the last grazing day. During the first 4 days, the avoidance index of
317 the brown goat is in average equal to 2. Then, it started decreasing and is in average equal to 0.96 during
318 the last 3 days. The white goat generally had the lower avoidance index, it is < 1 only during days 3, 4 and
319 5.

320 Over the entire grazing week, all the animals had an avoidance index > 1 . However, it is only 1.04 for
321 the white goat.

322 When comparing the weekly avoidance index between Try 1 and 2, it is increasing for all the animals.
323 The white goat increased its weekly avoidance index by 76%, and by 207%, 142%, 60% for the brown,
324 black and red goats.

325 It is interesting to note that the greater was the LAF value during Try 1, the greater was the increase in
326 the weekly avoidance index on Try 2. The Pearson correlation coefficient between the LAF on Try - 1 and
327 the increase in the weekly avoidance index on Try 2 is equal to 0.93.

328 **3.6 Larval exposure and level of infection**

329 The logarithm of the area under the curve of the FEC curve (LAF) against the exposure coefficient is
330 available figure 7.

331 It is hard to find a simple relationship between the LAF and the exposure coefficient. The LAF is between
332 10.5 and 11.2 for most of the exposure coefficient. It is important to note that similar exposure coefficient
333 can have different LAF. For example, the red goat had an exposure coefficient equal to 8,417 during Try

334 1, and it was equal to 8,374 for the black goat during Try 2. Even if their exposure coefficient were very
335 closed, their LAF are respectively the minimal and maximal observed value.

336 3.7 Social Distance

337 The distribution of the inter-individual distances are available in figure 8.

338 During the first Try, the inter-individual distance between the brown, black and red goats were
339 homogeneous, and in average equals to 3.7m. On the contrary, the white goat tends to be more distant from
340 the others. For the white goat, the average distance with the others is equal to 5.6m.

341 During the second Try, the white goat was still more distant from the other, but decreased the average
342 distance to 5m. On the contrary, the black goat slightly increases its inter-individual with the brown and
343 red goats. The inter-individual distance was equal to 3.8m during the first Try and increased to 4m during
344 the second Try.

4 DISCUSSION

345 We provided a conceptual framework to study the interaction between animal behavior and parasitism. It
346 is based on automatic animal monitoring using image analysis, to detect and identify the animals on the
347 images, allowing to record the spatial coordinates of the animals over time. We were able to derive several
348 interesting indicator, such that the avoidance index, the exposure index and the inter-individual distance.
349 We then studied the relationship between these indicators and the animals level of infection, which was
350 assessed with the FEC.

351 We showed that animals had heterogeneous avoidance capacity, which also varies with time. We observed
352 that avoidance capacity increases during the second try, for all animals. This could reveal the ability of
353 the animals to memorize the location of the infected areas. In addition, we observed that the more the
354 animals were infected during the first try, the more they increased their avoidance capacity during the
355 second try. For sheep, it has been shown that the avoidance capacity increases with the level of infection
356 (Hutchings et al., 1999; Cooper et al., 2000), similar mechanisms are maybe observed here. Some animals
357 had an avoidance capacity > 1 during the first grazing days, and then became < 1 for the rest of the week.
358 Several explanations can be proposed, such as the age of feces, which can decrease the avoidance capacity
359 (Hutchings et al., 1998). But also because animals naturally dropped feces inside the pasture, gradually
360 increasing the quantity of feces inside the non-infected area. This is a limitation of our study, and futur
361 works should use feces bag to avoid contaminating the non-infected area, as suggested in Hutchings et al.
362 (2001).

363 We were not able to distinguish a clear relationship between the larval exposure and the level of infection,
364 neither between the avoidance index and the level of infection. This suggest that larval intake is a random
365 process and is not directly proportional to the time spent on contaminated areas. Finally, we were not able
366 to find a clear relationship between the inter-individual distance and the infection level. The biological
367 interpretation resulting from our analysis should be interpreted with caution, due to the low number of
368 monitored animals.

369 However, our work provides interesting insights to develop routine studies that characterize the behavior
370 of animals and can be improved in different ways. First, our work could benefit from a daily estimation
371 of the number of larvae inside the infected areas, to improve the estimation of the exposure index. For
372 the second try, the larval population was possibly increasing after the third grazing day. However, we
373 were not able to observe this dynamic, as we only had an observation on the last grazing day. Second,

374 the performance of the animal detection and identification could also be improved. We used time-lapse
375 construction camera with a resolution of 1208 x 720 and 1.3 Mpx, which was convenient because it ran
376 on batteries and stored the image on a SD card for the entire grazing week. This is particularly adapted
377 to outdoor conditions, where the pasture can be located far from any facilities. However, using a camera
378 with higher definition can improve the details in the image, especially when the object are located far from
379 the camera, and thus potentially increase detection rate. Animal identification can be improved by using
380 video recording instead of images generated from time-lapse camera. With videos, animal identification
381 can benefit from object tracking technics (Li et al., 2021; van der Zande et al., 2021). With video, it could
382 be possible to estimate the speed and acceleration of the animals, and to classify its activity. Using color
383 marks on the animals can be an interesting solution to increase both the detection and identification method.
384 This color marks should be visible from the camera, no matter the animal posture and its angle from the
385 camera. Finally, as it is shown in this article, it is important to consider the sun trajectory when deciding
386 the camera location.

387 Most studies on small ruminant behavior rely on human observation. This is particularly time consuming,
388 and in general, observations are limited in time and frequency. Automatic monitoring will allow to acquire
389 long-term individual data, necessary to study the link between behavior and several aspect of animal health
390 and welfare. However, visual observation enables to compute useful information, such that the number of
391 bites (Hutchings et al., 1998), and to identify when the animal is eating or not. Futur development could
392 focus on tracking the animal head, and possibly detect when the animal head is in contact with grass.

CONFLICT OF INTEREST STATEMENT

393 The authors declare that the research was conducted in the absence of any commercial or financial
394 relationships that could be construed as a potential conflict of interest.

AUTHOR CONTRIBUTIONS

395 The Author Contributions section is mandatory for all articles, including articles by sole authors. If an
396 appropriate statement is not provided on submission, a standard one will be inserted during the production
397 process. The Author Contributions statement must describe the contributions of individual authors referred
398 to by their initials and, in doing so, all authors agree to be accountable for the content of the work. Please
399 see here for full authorship criteria.

FUNDING

400 The cameras were funded by the project suiRAvi, supported by the animal genetics division of INRAE.
401 The study was supported by Région Guadeloupe and the European Union Fund (FEDER) in the framework
402 of the AgroEcoDiv project.

ACKNOWLEDGMENTS

403 This is a short text to acknowledge the contributions of specific colleagues, institutions, or agencies that
404 aided the efforts of the authors.

SUPPLEMENTAL DATA

405 Supplementary Material should be uploaded separately on submission, if there are Supplementary Figures,
406 please include the caption in the same file as the figure. LaTeX Supplementary Material templates can be
407 found in the Frontiers LaTeX folder.

DATA AVAILABILITY STATEMENT

408 The datasets [GENERATED/ANALYZED] for this study can be found in the [NAME OF REPOSITORY]
409 [LINK].

REFERENCES

- 410 Achour, B., Belkadi, M., Filali, I., Laghrouche, M., and Lahdir, M. (2020). Image analysis for individual
411 identification and feeding behaviour monitoring of dairy cows based on convolutional neural networks
412 (cnn). *Biosystems Engineering* 198, 31–49
- 413 Andrew, W., Greatwood, C., and Burghardt, T. (2017). Visual localisation and individual identification
414 of holstein friesian cattle via deep learning. In *Proceedings of the IEEE International Conference on*
415 *Computer Vision (ICCV) Workshops*
- 416 Aschwanden, J., Gygax, L., Wechsler, B., and Keil, N. M. (2008). Social distances of goats at the feeding
417 rack: Influence of the quality of social bonds, rank differences, grouping age and presence of horns.
418 *Applied Animal Behaviour Science* 114, 116–131
- 419 Aumont, G., Pouillot, R., and Mandonnet, N. (1997). Le dénombrement des éléments parasitaires: Un outil
420 pour l'étude de la résistance génétique aux endo-parasites chez les petits ruminants. In *Workshop final*
421 *de l'AT CIRAD-MIPA*. vol. 72, 94
- 422 Barroso, F., Alados, C. L., and Boza, J. (2000). Social hierarchy in the domestic goat: effect on food habits
423 and production. *Applied Animal Behaviour Science* 69, 35–53
- 424 Bishop, S. and Stear, M. (2000). The use of a gamma-type function to assess the relationship between the
425 number of adult teladorsagia circumcincta and total egg output. *Parasitology* 121, 435–440
- 426 Bonneau, M., Bambou, J.-C., Mandonnet, N., Arquet, R., and Mahieu, M. (2018). Goats worm burden
427 variability also results from non-homogeneous larval intake. *Scientific reports* 8, 15987
- 428 Bonneau, M., Vayssade, J.-A., Troupe, W., and Arquet, R. (2020). Outdoor animal tracking combining
429 neural network and time-lapse cameras. *Computers and Electronics in Agriculture* 168, 105150
- 430 Brambilla, A., von Hardenberg, A., Kristo, O., Bassano, B., and Bogliani, G. (2013). Don't spit in the
431 soup: faecal avoidance in foraging wild alpine ibex, capra ibex. *Animal Behaviour* 86, 153–158
- 432 Charlier, J., Thamsborg, S. M., Bartley, D. J., Skuce, P. J., Kenyon, F., Geurden, T., et al. (2018).
433 Mind the gaps in research on the control of gastrointestinal nematodes of farmed ruminants and pigs.
434 *Transboundary and emerging diseases* 65, 217–234
- 435 Cooper, J., Gordon, I. J., and Pike, A. W. (2000). Strategies for the avoidance of faeces by grazing sheep.
436 *Applied Animal Behaviour Science* 69, 15–33
- 437 Cornell, S. J., Isham, V. S., and Grenfell, B. T. (2004). Stochastic and spatial dynamics of nematode
438 parasites in farmed ruminants. *Proceedings of the Royal Society of London. Series B: Biological Sciences*
439 271, 1243–1250
- 440 Fox, N. J., Marion, G., Davidson, R. S., White, P. C., and Hutchings, M. R. (2013). Modelling parasite
441 transmission in a grazing system: the importance of host behaviour and immunity. *PloS one* 8, e77996

- 442 Gan, H., Ou, M., Zhao, F., Xu, C., Li, S., Chen, C., et al. (2021). Automated piglet tracking using a single
443 convolutional neural network. *Biosystems Engineering* 205, 48–63
- 444 He, K., Zhang, X., Ren, S., and Sun, J. (2016). Deep residual learning for image recognition. In
445 *Proceedings of the IEEE Conference on Computer Vision and Pattern Recognition (CVPR)*
- 446 Hutchings, M., Kyriazakis, I., Gordon, I., and Jackson, F. (1999). Trade-offs between nutrient intake and
447 faecal avoidance in herbivore foraging decisions: the effect of animal parasitic status, level of feeding
448 motivation and sward nitrogen content. *Journal of Animal Ecology* 68, 310–323
- 449 Hutchings, M. R., Gordon, I. J., Kyriazakis, I., and Jackson, F. (2001). Sheep avoidance of faeces-
450 contaminated patches leads to a trade-off between intake rate of forage and parasitism in subsequent
451 foraging decisions. *Animal Behaviour* 62, 955–964
- 452 Hutchings, M. R., Judge, J., Gordon, I. J., Athanasiadou, S., and Kyriazakis, I. (2006). Use of trade-off
453 theory to advance understanding of herbivore–parasite interactions. *Mammal Review* 36, 1–16
- 454 Hutchings, M. R., Kyriazakis, I., Anderson, D., Gordon, I. J., and Coop, R. (1998). Behavioural strategies
455 used by parasitized and non-parasitized sheep to avoid ingestion of gastro-intestinal nematodes associated
456 with faeces. *Animal Science* 67, 97–106
- 457 Jiang, M., Rao, Y., Zhang, J., and Shen, Y. (2020). Automatic behavior recognition of group-housed goats
458 using deep learning. *Computers and Electronics in Agriculture* 177, 105706
- 459 Kaplan, R. M. and Vidyashankar, A. N. (2012). An inconvenient truth: global worming and anthelmintic
460 resistance. *Veterinary parasitology* 186, 70–78
- 461 Li, G., Huang, Y., Chen, Z., Chesser, G. D., Purswell, J. L., Linhoss, J., et al. (2021). Practices and
462 applications of convolutional neural network-based computer vision systems in animal farming: A review.
463 *Sensors* 21, 1492
- 464 Louie, K., Vlassoff, A., and Mackay, A. (2005). Nematode parasites of sheep: extension of a simple model
465 to include host variability. *Parasitology* 130, 437–446
- 466 Marsot, M., Mei, J., Shan, X., Ye, L., Feng, P., Yan, X., et al. (2020). An adaptive pig face recognition
467 approach using convolutional neural networks. *Computers and Electronics in Agriculture* 173, 105386
- 468 Qiao, Y., Su, D., Kong, H., Sukkarieh, S., Lomax, S., and Clark, C. (2019). Individual cattle identification
469 using a deep learning based framework. *IFAC-PapersOnLine* 52, 318–323
- 470 Redmon, J. and Farhadi, A. (2017). Yolo9000: better, faster, stronger. In *Proceedings of the IEEE*
471 *conference on computer vision and pattern recognition*. 7263–7271
- 472 Rose, H., Wang, T., van Dijk, J., and Morgan, E. R. (2015). Gloworm-fl: a simulation model of the
473 effects of climate and climate change on the free-living stages of gastro-intestinal nematode parasites of
474 ruminants. *Ecological Modelling* 297, 232–245
- 475 Saccareau, M., Moreno, C., Kyriazakis, I., Faivre, R., and Bishop, S. (2016). Modelling gastrointestinal
476 parasitism infection in a sheep flock over two reproductive seasons: in silico exploration and sensitivity
477 analysis. *Parasitology* 143, 1509–1531
- 478 Su, Q., Tang, J., Zhai, J., Sun, Y., and He, D. (2021). Automatic tracking of the dairy goat in the surveillance
479 video. *Computers and Electronics in Agriculture* 187, 106254
- 480 Szegedy, C., Vanhoucke, V., Ioffe, S., Shlens, J., and Wojna, Z. (2016). Rethinking the inception
481 architecture for computer vision. In *Proceedings of the IEEE Conference on Computer Vision and*
482 *Pattern Recognition (CVPR)*
- 483 Ungerfeld, R. and Correa, O. (2007). Social dominance of female dairy goats influences the dynamics of
484 gastrointestinal parasite eggs. *Applied Animal Behaviour Science* 105, 249–253

- 485 van der Zande, L. E., Guzhva, O., and Rodenburg, T. B. (2021). Individual detection and tracking
 486 of group housed pigs in their home pen using computer vision. *Frontiers in Animal Science* 2, 10.
 487 doi:10.3389/fanim.2021.669312
- 488 Wang, D., Tang, J., Zhu, W., Li, H., Xin, J., and He, D. (2018). Dairy goat detection based on faster r-cnn
 489 from surveillance video. *Computers and Electronics in Agriculture* 154, 443–449
- 490 Yang, A., Huang, H., Yang, X., Li, S., Chen, C., Gan, H., et al. (2019). Automated video analysis of
 491 sow nursing behavior based on fully convolutional network and oriented optical flow. *Computers and*
 492 *Electronics in Agriculture* 167, 105048
- 493 Zhang, Y., Cai, J., Xiao, D., Li, Z., and Xiong, B. (2019). Real-time sow behavior detection based on deep
 494 learning. *Computers and Electronics in Agriculture* 163, 104884
- 495 Zheng, C., Yang, X., Zhu, X., Chen, C., Wang, L., Tu, S., et al. (2020). Automatic posture change analysis
 496 of lactating sows by action localisation and tube optimisation from untrimmed depth videos. *Biosystems*
 497 *Engineering* 194, 227–250
- 498 Zitova, B. and Flusser, J. (2003). Image registration methods: a survey. *Image and vision computing* 21,
 499 977–1000

TABLES

	Try - 1			Try - 2		
	ZI 1	ZI 2	ZNI	ZI 1	ZI 2	ZNI
Start	8cm	8.3cm	7.32cm	10.8cm	9.3cm	10.7cm
End	5.05cm	6cm	4.8cm	6.4cm	7.3cm	5.5cm
Δ	-36.9%	-27.1%	-34.4%	-40.7%	-21%	-47.7%

Table 1. Sward height when grazing started and ended. The last row gives the height different, in percentage, between start and end.

	Pct Detection - Try 1	Pct detection - Try 2
White	95%	95%
Brown	78%	80.8%
Black	84.3%	91.5%
Red	86.8%	92.1%
Average	86%	89.9%

Table 2. Percentage of detection of the animal detection method. The average is computed over all color classes.

	Try 1	Sensitivity	Precision	Try 2	Sensitivity	Precision
White		98.9%	95.7%		99%	97.6%
Brown		95.9%	85.9%		94.4%	94.1%
Black		89.4%	95.7%		94.2%	96.7%
Red		92%	97.6%		95.7%	95.1%
Average		94%	93.7%		95.8%	95.9%

Table 3. Sensitivity and precision of the animal identification method. The average is computed over all color classes.

FIGURE CAPTIONS

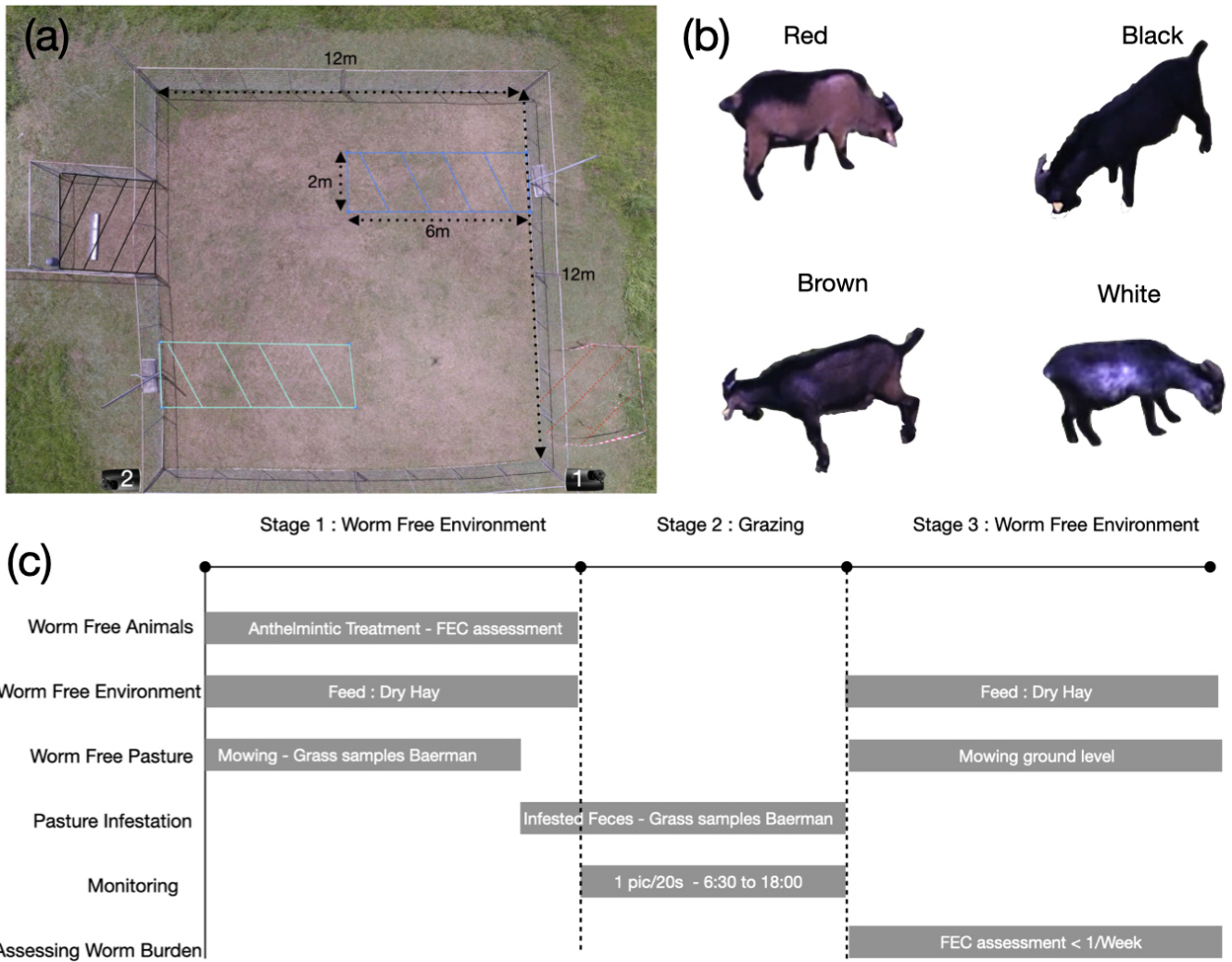


Figure 1. (a) Pasture setup. The blue and green dashed areas are the two infected areas. The black dashed square is the resting area. During experiment, we placed a sheet of metal inside the area to produce shade. The red area is the control area, to estimate the number of infected larvae on pasture. During Try 2, the control area was located on the opposite side of pasture. On Try 1, we used the camera located on the bottom right corner of the pasture and on the bottom right on Try 2. (b) Picture example of the four Creole goats used during the experiment. (c) Schematic representation of the experiment.

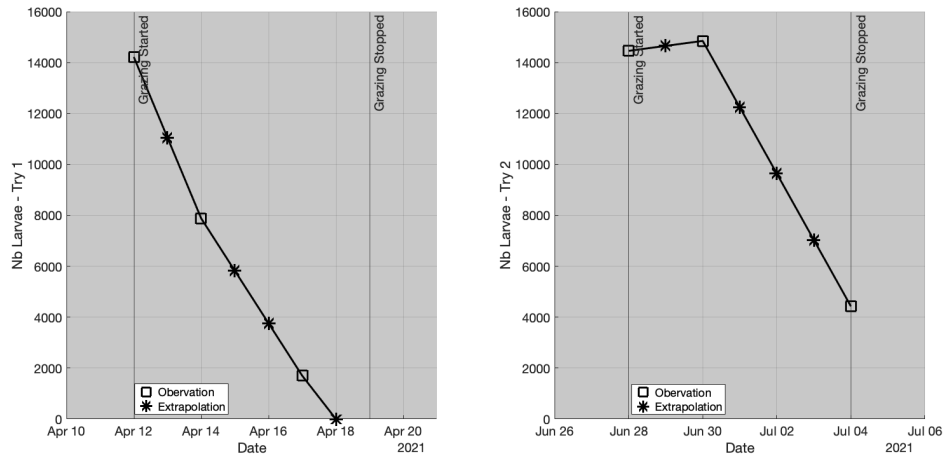


Figure 2. Estimated number of larvae inside each infected areas for Try 1 (left) and Try 2 (right). We used square mark when the number of larvae was estimated from the control samples, and star mark when it was extrapolated from the observations.

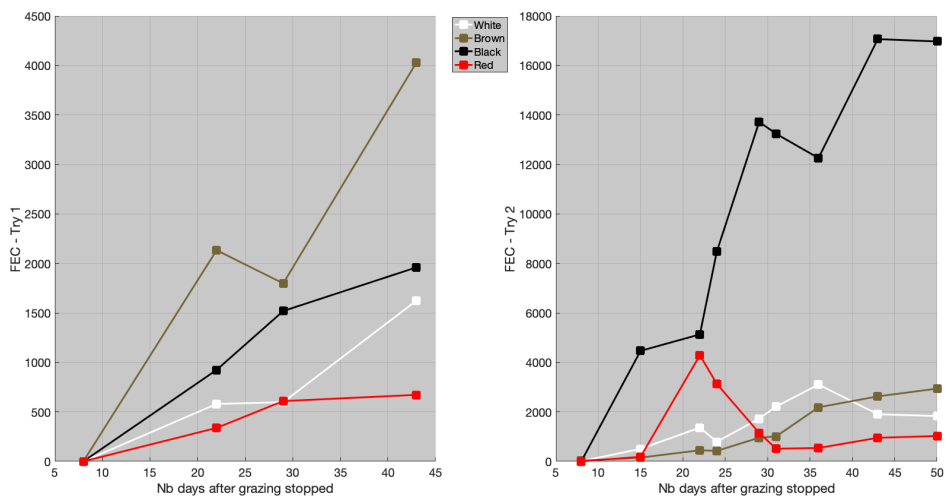


Figure 3. Individual fecal egg count (FEC), in eggs/g of feces, for Try 1 (left) and Try 2 (right).

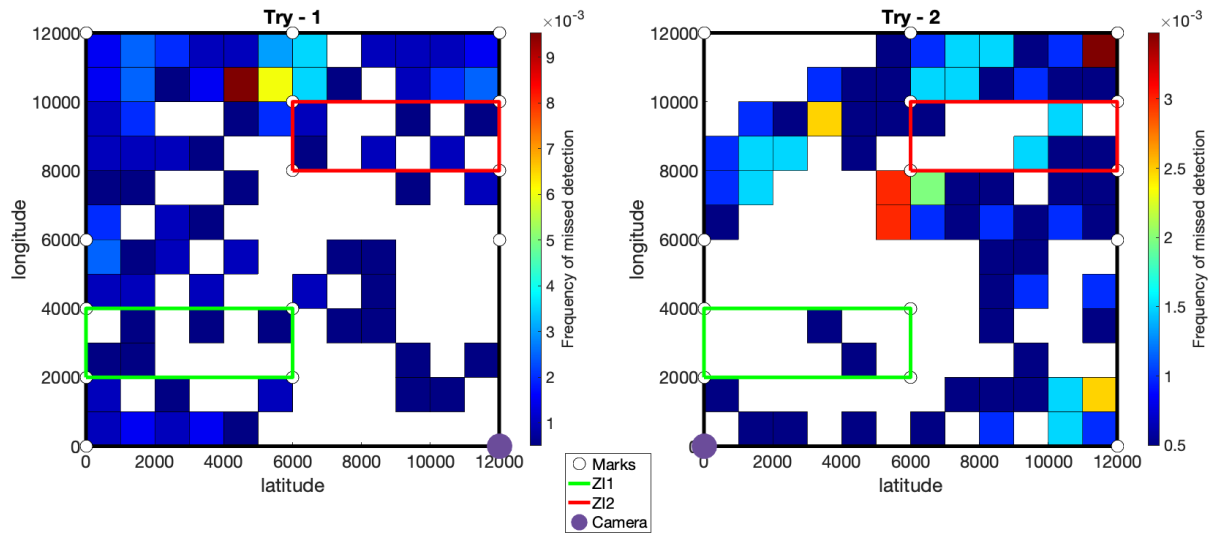


Figure 4. Spatial frequency of missed detections. The pasture is delimited by the black lines. The green and red lines define the first and second infected areas. The white disks provide the locations of the marks used to fit the geometric transformation from pixels to spatial coordinates. For each try, the location of the camera is defined by the purple disk.

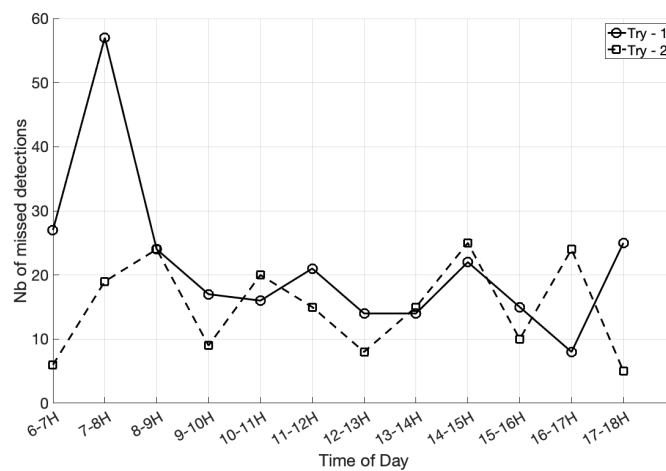


Figure 5. Number of missed detection as a function of time of the day, for Try 1 and Try 2.

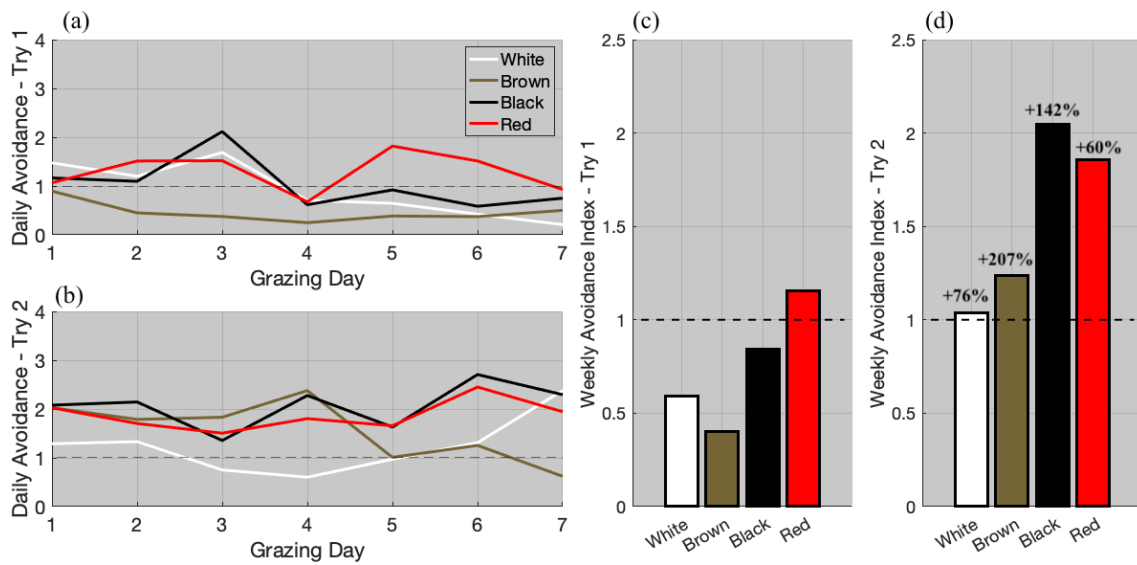


Figure 6. Avoidance index. (a) Daily avoidance index for Try - 1 and (b) for Try - 2. (c) Cumulated avoidance index for Try - 1 and (d) for Try - 2. For Try - 2, we provided the percentage of increase compared to Try -1.

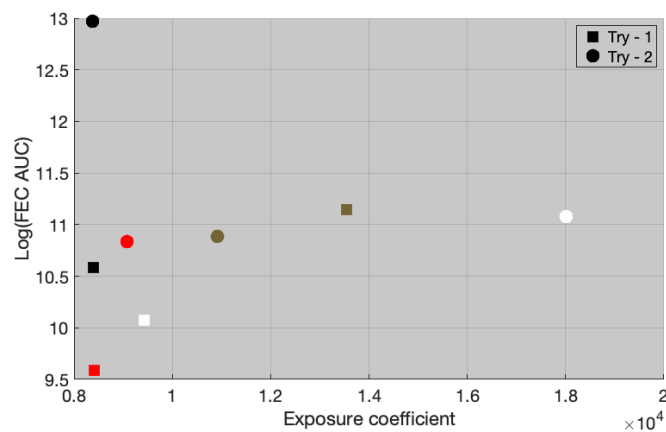


Figure 7. Logarithm of the area under the curve (AUC) of the FEC curve against the exposure coefficient.

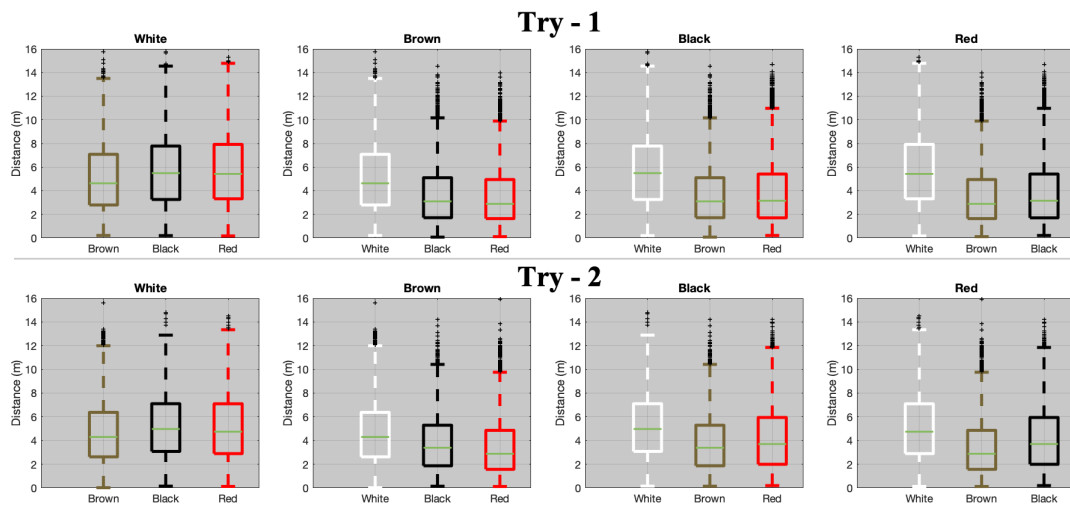


Figure 8. Box-plot of the inter-individual distances in Try 1 (top) and Try 2 (bottom). Each title provides the studied animal and the three box-plots provides the distance distribution between this animal and the three other animals. For example, the three box-plots on the top left corner provides the inter-individual distance between the white goat, and the brown, black and red goat during Try 1.